Available online at www.sciencedirect.com

ScienceDirect

Procedia CIRP 00 (2019) 000–000

www.elsevier.com/locate/procedia

17th CIRP Conference on Modelling of Machining Operations

Cutting Force Prediction in Robotic Machining

Edouard Rivière-Lorphèvre[a,*], Hoai Nam Huynh[b], Francois Ducobu[a], Olivier Verlinden[b]

[a] University of Mons, Machine Design and Manufacturing Department, Place du Parc 20, B-7000 Mons, Belgium
[b] University of Mons, Theoretical Mechanics, Dynamics an Vibrations Department, Place du Parc 20, B-7000 Mons, Belgium

Abstract

Modelling of cutting forces in milling is a key aspect for an accurate simulation of the process. For fast and reliable simulation with 3 axis milling machines, macroscopic approach is often used. The tool is divided in slices around its axis and a mechanistic model is used to predict the elementary cutting forces. In robotic machining, the tool can experience more complex toolpath and its axis may be tilted during machining due to the flexibility of the robot. The paper presents an improvement of the cutting forces model allowing the simulation for cases where the degrees of freedom in rotation of the axis are freed.

Peer-review under responsibility of the scientific committee of The 17th CIRP Conference on Modelling of Machining Operations, in the person of the Conference Chair Dr Erdem Ozturk and Co-chairs Dr Tom Mcleay and Dr Rachid Msaoubi.

Keywords: Machining; Robot; Simulation

1. Introduction

Robotic machining is a new development opening interesting possibilities from an industrial point of view. As compared to traditional CNC milling machines, robots offers a larger working range and a better accessibility. However, the serial architecture of the robot makes it prone to vibratory problems such as chatter [1]. The optimisation of the whole process (toolpath, robot posture, cutting parameters) can be acchieved from an experimental point of view [2, 3] but the tests are time consuming and needs to be supported by physical modelling.
Numerical simulation is a promising approach to optimize the machining operation on a robot. The main idea is to generalize the time-domain methods developed for a classical machine-tool[4] to the specificities of robotic machining. Three aspects must be considered in the model: the dynamic behaviour of the robot[5, 6], the cutting forces produced by the mill[7] and the removal of the material from the workpiece [8, 9]. Several aspects makes the simulation more complex with a robot than with a standard CNC machine:

- Like in five axis milling, the movement of the tool combines translation an rotation of the bodies; therefore, the geometrical modelling of the removal of material is more complex than for 2D1/2 operations;
- the dynamic response of the robot depend on the position of the end effector and the configuration of the robot;
- flexibilities of the bodies and the joints can have an impact on the flexibility of the system, the control can also have an influence on the stability of the system.

2. Objective of the paper

The aim of the paper is to describe the generalization of an eraser of matter model used to predict the machined surface for milling operation. The rotational degrees of freedom are set free in order to allow a more accurate simulation of robotic machining without adding too much complexity in this stage of the simulation.

3. General algorithm

The dynamic behavior of the robot can be modelled by its modal model [7, 5, 6] or via multibody approach [10, 11]. Both approaches allow the setting of the model of motion described by the governing equation:

* Corresponding author. Tel.: +3265374547.
E-mail address: edouard.riviere@umons.ac.be (Edouard Rivière-Lorphèvre).

Peer-review under responsibility of the scientific committee of The 17th CIRP Conference on Modelling of Machining Operations, in the person of the Conference Chair Dr Erdem Ozturk and Co-chairs Dr Tom Mcleay and Dr Rachid Msaoubi.

$$\mathbf{M}\left(\underline{\mathbf{q}}\right)\cdot\underline{\ddot{\mathbf{q}}}+\underline{\mathbf{h}}\left(\underline{\mathbf{q}},\underline{\dot{\mathbf{q}}}\right)=\underline{\mathbf{g}}\left(\underline{\mathbf{q}},\underline{\dot{\mathbf{q}}},t\right) \quad (1)$$

where $\underline{\mathbf{q}}$ is the vector gathering the configuration parameters of the system, $\underline{\dot{\mathbf{q}}}$ and $\underline{\ddot{\mathbf{q}}}$ its first and second time derivatives, $\mathbf{M}$ the mass matrix, $\underline{\mathbf{h}}$ the contribution of centrifugal, gyroscopic and Coriolis effects and $\underline{\mathbf{g}}$ the external forces [12].
These equations can be rewritten as:

$$\mathbf{M}\left(\mathbf{q}\right)\cdot\underline{\ddot{\mathbf{q}}}+\underline{\mathbf{H}}\left(\underline{\mathbf{q}},\underline{\dot{\mathbf{q}}},t\right)=f\left(\underline{\mathbf{q}},\underline{\dot{\mathbf{q}}},\underline{\ddot{\mathbf{q}}},t\right)=0 \quad (2)$$

with $\underline{\mathbf{H}}\left(\underline{\mathbf{q}},\underline{\dot{\mathbf{q}}},t\right)=\underline{\mathbf{h}}\left(\underline{\mathbf{q}},\underline{\dot{\mathbf{q}}}\right)-\underline{\mathbf{g}}\left(\underline{\mathbf{q}},\underline{\dot{\mathbf{q}}},t\right)$.

In order to solve these equations numerically, the total time of the simulation is divided in small increments (time step h) and each part of equation 2 is evaluated at each time step. The computation of position and velocity from the acceleration is made by choosing and integration scheme allowing the prediction of position and speed at the next time step from the value of position, velocity and acceleration at the current time step and the acceleration at the next time step:

$$\underline{q}^{t+h}=\underline{\mathbf{\Lambda}}\left(\underline{\mathbf{q}}^{t},\underline{\dot{\mathbf{q}}}^{t},\underline{\ddot{\mathbf{q}}}^{t},\underline{\ddot{\mathbf{q}}}^{t+h}\right) \quad (3)$$

$$\underline{\dot{q}}^{t+h}=\underline{\tilde{\mathbf{\Lambda}}}\left(\underline{\mathbf{q}}^{t},\underline{\dot{\mathbf{q}}}^{t},\underline{\ddot{\mathbf{q}}}^{t},\underline{\ddot{\mathbf{q}}}^{t+h}\right) \quad (4)$$

$\underline{\mathbf{\Lambda}}$ and $\underline{\tilde{\mathbf{\Lambda}}}$ are the expression of position and speed at the next time step as a function of the acceleration. The choice of Newmark's scheme [13] gives good results for milling operations. The equations of motion are then built in their residual form from the kinematics and the applied forces. The integration consists in computing the equations of motion (equation 2) in terms of the accelerations at time $t+h$ after having replaced the positions q (equation 3) and the velocities $\dot{q}$ (equation 4) by their integration formulas. With this substitution, the only remaining unknowns are the accelerations $\ddot{q}$:

$$\begin{aligned} f\left(\underline{\mathbf{q}}^{t+h}),\underline{\dot{\mathbf{q}}}^{t+h},\underline{\ddot{\mathbf{q}}}^{t+h}\right) &= \\ f\left(\underline{\mathbf{\Lambda}}\left(\underline{\mathbf{q}}^{t},\underline{\dot{\mathbf{q}}}^{t},\underline{\ddot{\mathbf{q}}}^{t},\underline{\ddot{\mathbf{q}}}^{t+h}\right),\underline{\tilde{\mathbf{\Lambda}}}\left(\underline{\mathbf{q}}^{t},\underline{\dot{\mathbf{q}}}^{t},\underline{\ddot{\mathbf{q}}}^{t},\underline{\ddot{\mathbf{q}}}^{t+h}\right),\underline{\ddot{\mathbf{q}}}^{t+h}\right) &= \\ \underline{\mathbf{F}}\left(\underline{\ddot{\mathbf{q}}}^{t+h}\right)=0 \end{aligned} \quad (5)$$

The solution of this equation is found using a zero-finding procedure to achieve the convergence of the acceleration $\ddot{\mathbf{q}}$ for each configuration parameter at time $t+h$ as. Newton-Raphson method can be chosen, leading to:

$$\underline{\ddot{\mathbf{q}}}^{t+h,n}=\underline{\ddot{\mathbf{q}}}^{t+h,n-1}-\mathbf{J}^{-1}\cdot\underline{\mathbf{F}}\left(\underline{\ddot{\mathbf{q}}}^{t+h,n-1}\right) \quad (6)$$

with n the iteration on the Newton Raphson procedure, $\underline{\mathbf{F}}\left(\underline{\ddot{\mathbf{q}}}^{t+h}\right)$ the equation of motion and $\mathbf{J}$ the Jacobian matrix of equation 5 with respect to the unknown accelerations. Convergence is obtained when:

$$\left\|\underline{\ddot{\mathbf{q}}}^{t+h,n}-\underline{\ddot{\mathbf{q}}}^{t+h,n-1}\right\|\leq\epsilon \quad (7)$$

with ϵ the tolerance. During the numerical integration of the equations of motion, the first predicted position of the cutting edge is only determined by considering the kinematics of the machine. A corrected position can be found by taking the dynamics of the system into account (Figure 1). This leads to a slightly different position of the cutting edges, modifying accordingly the value of the cutting force. The cutting force evaluated at the beginning of the time step can be updated, leading to a new estimation of the position of the cutting edge. The computation of a single time step thus needs to iterate the intersection procedure until the position of the cutting edge has converge within a given tolerance. Once the convergence is achieved, the surface is updated before the computation of the next time step.

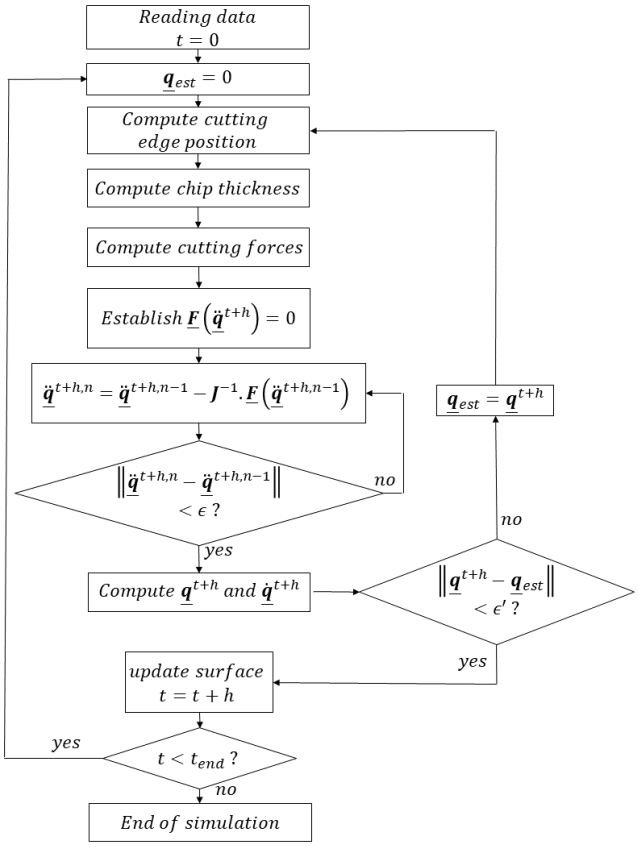

Fig. 1. General algorithm.

3.1. Surface modelling

One of the key aspect in the dynamic simulation of milling is the prediction of the interaction between the tool and the workpiece. This part of the algorithm allows the prediction of the cutter engagement, the undeformed chip thickness and the updated surface allowing the prediction of the kinematic roughness.
For a full 3D operation, the literature presents models based on CAD approach such as triangular mesh [8, 9], voxel [14, 15], dexel [16] or complex engagement identification [17]. The aim of this paper is to present a simplified approach based on the extension of an eraser of matter model [18].

3.1.1. Eraser of matter model

In this model the surface is seen as a stack of slices, each of them described by a set of interconnected points. The movement of the cutting edge in each slice is followed (figure 2). During each time step, the movement of the cutting edge is approximated by a polynomial function (Peigne et al [18] shows that a second order curve gives a good compromise between accuracy and computing time). The distance between the current position of the cutting edge and the intersection of the action line with the surface gives the undeformed chip thickness.

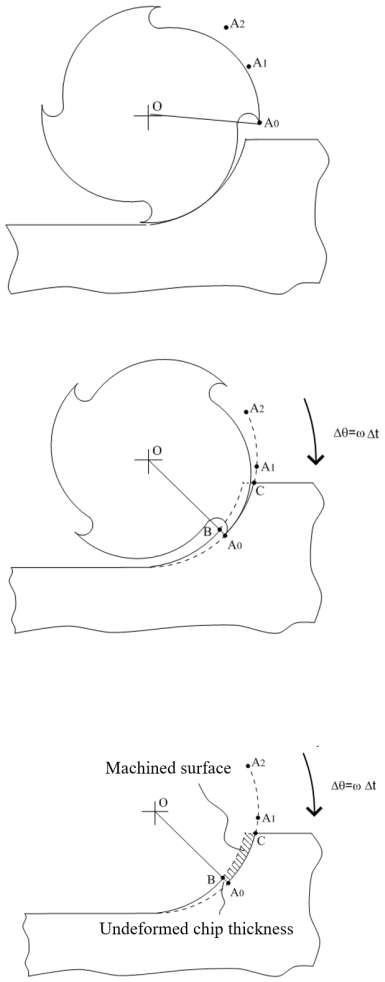

Fig. 2. Eraser of matter model (O: cutter center; A_0, A_1, A_2: position of the cutting edge at time t, $t-1$ and $t-2$; B: intersection of line $0A_0$ with the surface; C: intersection of edges path with the surface.

After convergence of the dynamic system, the area swept by the cutting edge during the time step is removed from the surface in order to update it. By following the value of the undeformed chip thickness between two time steps, it is possible to determine the type of option to consider (figure 3):

- if no contact between tool and workpiece was detected at previous time step:
  - if there is still no contact, no machining is made and the surface doesn't need to be updated;
  - if a contact is detected, the cutting edge enters into the workpiece.
- if the cutting edge was machining during the previous time step:
  - if a contact is still present, the machining carries on;
  - if the contact is lost, the cutting edge exits the workpiece.

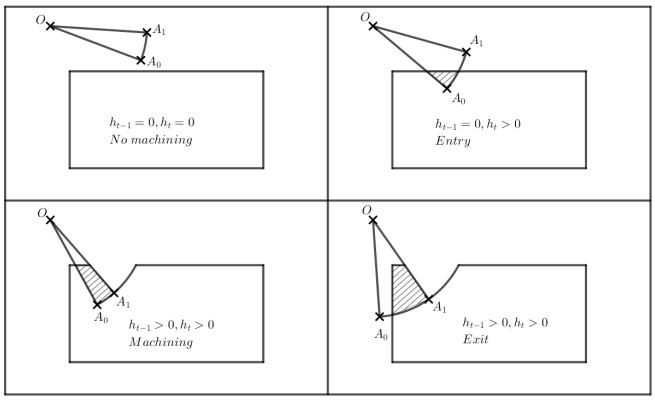

Fig. 3. Eraser of matter model.

3.1.2. Cutting edge modelling

Engin et al [19] proposed a procedure to evaluate the geometrical data (radius, orientation of the cutting edge,...) for any kind of standard solid endmill on a frame attached to the cutter itself. In order to allow a complex movement of the cutter during the simulation, it is necessary to transform the coordinates of all the points describing the cutting tool movement. For this purpose, three geometrical operations described by their respective homogeneous transformation matrices are successfully performed to obtained the final position of the edge:

- a rotation around the axis of the cutter of an angle $\theta = \omega \cdot t$;
- a translation to take the nominal feed of the cutter into account;
- the deviation of the cutter (in translation and rotation) due to the vibration of the cutter.

The classical use of this model considers that the cutting tool has a planar motion, so one particular point on a cutting edge stays at the same height with respect to the surface.

3.1.3. 3D operations

The planar motion of the tool, which is a reasonable assumption for 2D1/2 milling operation is not valid any more for a robotic machining operation. Indeed, the flexibility of the robot joint and bodies may lead to a rotation of the axis of the spindle from its programmed position.
The proposed algorithm is described as follow:

- in order to optimize the computation, the geometrical data of the cutter are pre computed at the beginning of the simulation with a fine axial increment;
- this actual edge geometry is approximated by a Bezier spline [20] thank to the identification of poles P_i;
- the homogeneous transformation matrix (combining rotation of the cutter around its axis, feed motion and displacement or rotation of the cutter due to the flexibility) are applied to the poles;
- the intersection between the cutting edge and the surface is performed;
- the cutting forces are computed on a frame attached to the cutting tool and then projected on a global frame tanks to the homogeneous transformation matrix.

The coordinates of the points on a spline are computed by the blending of the poles by polynomial functions $B_{i,n}$:

$$C(u) = \sum_{i=0}^{n} B_{i,n}(u) P_i \; 0 \leq u \leq 1 \tag{8}$$

For Bezier curves, the blending functions are the nth degree Bernstein polynomials defined as:

$$B_{i,n}(u) = \frac{n!}{i!(n-i)!} u^i (1-u)^{n-i} \tag{9}$$

One interesting property used here is that the image of a Bezier curve by any affine transformation is the Bezier curve based on the poles that have been subjected to the affine transformation.

The choice of the number of poles is made at the beginning of the simulation to guarantee a maximal deviation between the actual cutting edge shape and its approximation below a given tolerance. For a cutter with a standard geometry, 10 poles are sufficient to limit the maximum deviation to 1 μm.

3.2. Cutting force modelling

Once the undeformed chip thickness has been computed, the elementary cutting force can be computed based on a mechanistic model. Several models are listed in the litterature, three of them are used by most authors: the linear model derived from Merchant's theory, the exponential model proposed by Kienzle[5] and the model proposed by Armarego [21].
The linear model considers that the elementary cutting force dF depend on the undeformed chip thickness h and the elementary axial depth of cut da via a proportional coefficient K (called the cutting coefficient or the specific pressure):

$$dF = K \cdot h \cdot da \tag{10}$$

The exponential model considers that the influence of the undeformed chip thickness is a power law (with the exponent n below one):

$$dF = K \cdot h^n \cdot da \tag{11}$$

The third model considers that the forces are produced by two main mechanisms: shearing of the chip (force proportional to undeformed chip section $h \cdot da$ and parameter K_c) and friction of the chip along cutting edge (proportional to elementary length of cutting edge dS and coefficient K_e):

$$dF = K_c \cdot h \cdot da + K_e \cdot dS \tag{12}$$

4. Simulation results

4.1. Cutting forces with an untilted cutter

A first test is performed to see if the model is able to reproduce results from the litterature [19]. Slot milling is made in GGG70 spheroidal graphite with a ball endmill of 12 mm diameter. The cutting parameters are a spindle speed of 1000 RPM, an axial depth of cut of 2 mm and a feed of 0.08 mm/tooth. The predicted cutting forces (figure 4) are identical to the reference, the proposed simulation method is thus able to correctly predict the cutting force for an operation without tilt of the cutter.

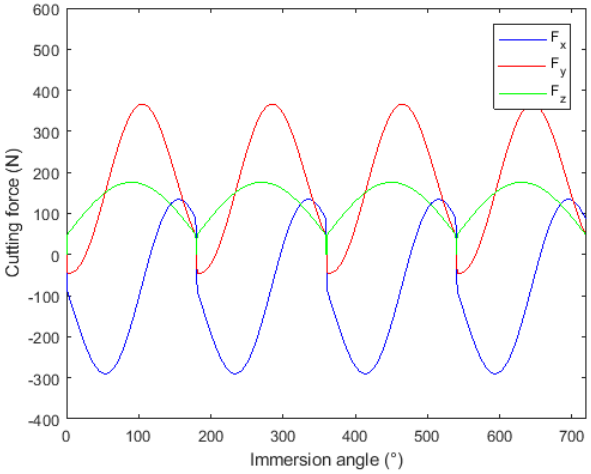

Fig. 4. Cutting force simulation with a ball endmill.

4.2. Constant tilt

For the next simulation, a cylindrical endmill of 10 mm diameter with four cutting edges is used. The machined material is 7075-T6 aluminum. A linear model is used for the cutting force with K_t=550 MPa and K_r=200 MPa [22]. The spindle speed is 20000 RPM, the feed per tooth is 0,05 mm, the radial depth of cut is 1 mm and the axial depth of cut 20 mm. The global frame is composed of x describing feed direction, z vertical and y creating an orthogonal frame xyz.
A constant tilt angle around x axis is imposed, varying from one to five degrees. Figures 5 and 6 shows the evolution of the cutting force on the x and y direction for two consecutive edges of the tool. It can be seen that the tilt of the cutter has a slight effect on the value of the cutting force but creates a significant modification of the immersion angle of the cutter. Indeed, for the five degree case, the radial depth of cut at the top of the cutter is more than the double of its nominal value.

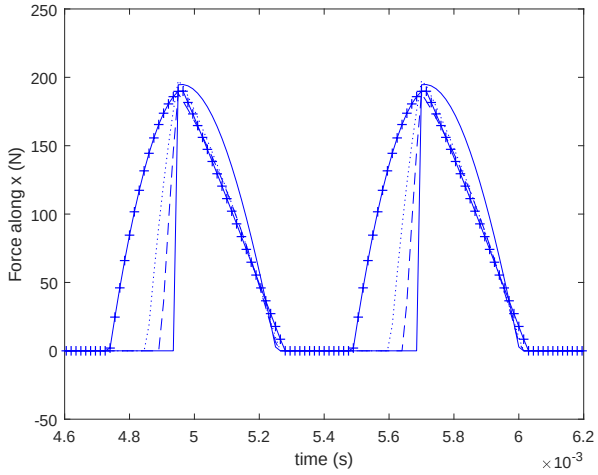

Fig. 5. x component of cutting force for 0 (plain), 1 (dashed), 2 (dotted) and 5 (plain with cross) degree tilt.

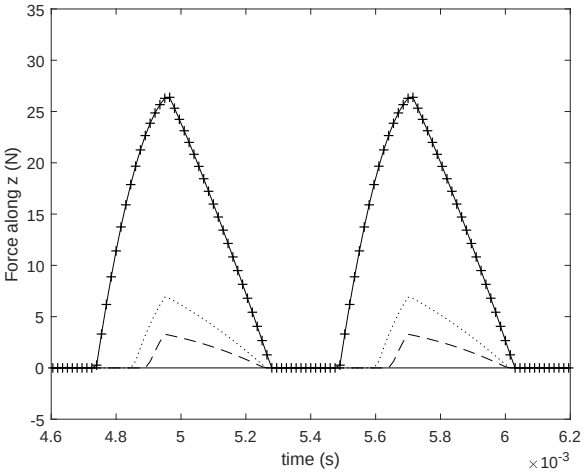

Fig. 7. z component of cutting force for 0 (plain), 1 (dashed), 2 (dotted) and 5 (plain with cross) degree tilt.

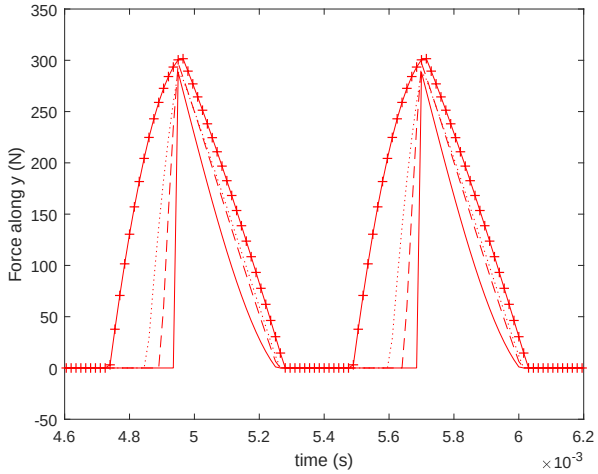

Fig. 6. y component of cutting force for 0 (plain), 1 (dashed), 2 (dotted) and 5 (plain with cross) degree tilt.

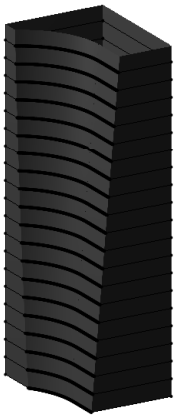

Fig. 8. Modelled surface for a constant tilt of 5 degree.

Tilt angle has a more significant effect on the value of the axial component (figure 7). Without tilt angle, the axial component is nearly zero while its value gradually increase with the tilt of the cutter.

The machined surface with 5° tilt angle is shown in figure 8.

4.3. Variable tilt

In order to show the effect of a time varying tilt on the cutter, a 10 mm ball endmill is used to model the cutting forces. The tilt angle has a sinusoidal variation at low frequency:

$$tilt = \alpha \cdot \sin(2\pi \cdot f \cdot t) \tag{13}$$

where α is the amplitude of the tilt variation and f the frequency of the oscillations. The specific pressures are the same as the previous case, a half immersion radial depth of cut is selected while the other cutting parameters are maintained (20 mm axial depth of cut, 0,05 mm/tooth feed, 20000 RPM spindle speed). The frequency imposed for the tilt is 10 Hz and its maximum value 5°. Figure 9 shows the evolution of the norm of the cutting force along the simulation. It can be seen that the envelope of the signal has a periodic evolution at the same frequency as the modulation of the tilt angle. This is the image of the evolution of the effective axial depth of cut during the simulation.

In addition, figure 10 shows the machined surface. The marks left by the tool are clearly visible in the workpiece.

5. Conclusion and perspectives

The paper presents the generalisation of a 2D1/2 approach to compute the cutting forces in milling if the cutting tool axis is tilted. The interaction between the tool and the workpiece is modelled thanks to an eraser of matter model allowing to

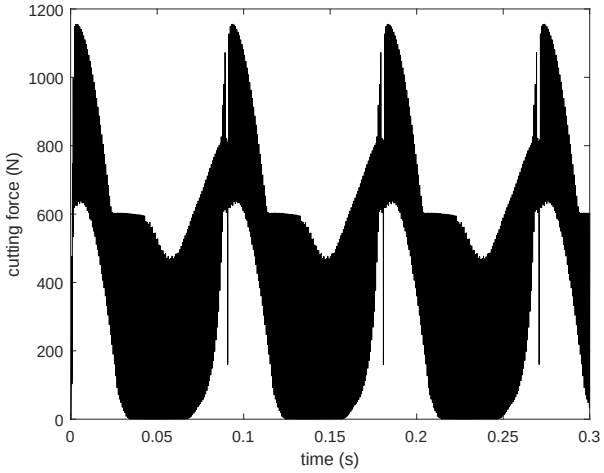

Fig. 9. Cutting force norm for the variable titl case.

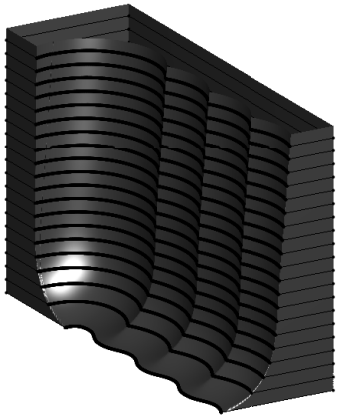

Fig. 10. Modelled surface for a variable tilt.

reduce the geometrical computations to plane cases. The proposed model is able to reproduce the machined surface and the cutting forces for translation and rotation of the cutter along its nominal position.

As a perspective, this model can be use to predict more accurately the cutting forces and the stability of milling operations on multi axis machines or robotic machining.

References

[1] M. Cordes, W Hintze, and Y. Altintas. Chatter stability in robotic milling. *Robotics and Computer Integrated Manufacturing*, 55:11–18, 2019.

[2] A. Klimchik, A. Ambiehl, S. Garnier, B. Furet, and A. Pashkevich. Experimental study of robotic-based machining. *IFAC Papers Online*, 49(12):174–179, 2016.

[3] Yang Lin, Huan Zhao, and Han Ding. Spindle configuration analysis and optimization considering the deformation in robotic machining applications. *Robotics and Computer Integrated Manufacturing*, 54:83–95, 2018.

[4] Y. Altintas. *Manufacturing Automation: Metal Cutting Mechanics, Machine Tool Vibrations, and CNC Design. 2nd Edition*. Cambridge University Press, 2012.

[5] B. Denkena, B. Bergmann, and T. Lepper. Design and optimisation of a machining robot. *Procedia Manufacturing*, 14:89–96, 2017.

[6] S. Garnier, K. Subrin, and K. Waiyagan. Modelling of robotic drilling. *Procedia CIRP*, 58:416–421, 2017.

[7] L. Cen and S. N. Melkote. Effect of robot dynamics on the machining forces in robotic milling. *Procedia Manufacturing*, 10:486–496, 2017.

[8] T. Siebrecht, P. Kersting, D. Biermann, S. Odendahl, and J. Bergmann. Modeling of surface location errors in a multi-scale milling simulation system using a tool model based on triangle meshes. *Procedia CIRP*, 37:188–192, 2015.

[9] X. Gong and H.-Y. Feng. Cutter-workpiece engagement determination for general milling using triangle mesh modeling. *Journal of Computational Design and Engineering*, 3:151–160, 2016.

[10] H. N. Huynh, G. Kouroussis, O. Verlinden, and E. Riviere. Modal updating of a 6-axis robot for milling application. In *Proceedings of the 25th International Congress on Sound and Vibration (ICSV25)*, 2018.

[11] H. N. Huynh, E. Riviere, and O. Verlinden. Multibody modelling of a flexible 6-axis robot dedicated to robotic machining. In *The 5th Joint International Conference on Multibody System Dynamics*, 2018.

[12] Kouroussis G., Rustin C., Bombled Q., and Verlinden O. Easydyn: multibody open-source framework for advanced research purposes. In *ECCOMAS Multibody Dynamics 2011*, 2011.

[13] E. Rivière-Lorphèvre, H. N. Huynh, and O. Verlinden. Influence of the time step selection on dynamic simulation of milling operation. *International Journal of Advanced Manufacturing Technology*, 95(9–12):4497–4512, 2018.

[14] P. Klimant, M. Witta, and M. Kuhla. Cad kernel based simulation of milling processes. *Procedia CIRP*, 17:710–715, 2014.

[15] O. Yousefian and J. A. Tarbutton. Prediction of cutting force in 3-axis cnc milling machines based on voxelization framework for digital manufacturing. *Procedia Manufacturing*, 1:512–521, 2015.

[16] B. Tukora and T. Szalay. Multi-dexel based material removal simulation and cutting force prediction with the use of general-purpose graphics processing units. *Advances in Engineering Software*, 43:65–70, 2012.

[17] Z. C. Wei, M. L. Guo, M. J. Wang, S. Q. Li, and S. X. Liu. Force predictive model for five-axis ball end milling of sculptured surface. *The International Journal of Advanced Manufacturing Technology*, 98:1367–1377, 2018.

[18] G. Peigne and Al. A model of milled surface generation for time domain simulation of high-speed cutting. *Proc. Instn Mech. Engrs Part B: J Engineering Manufacture*, 217 Number 7:919–930, July 2003.

[19] S. Engin and Y. Altintas. Mechanics and dynamics of general milling cutters. part I: Helical end mills. *Int. J. Mach. Tools Manuf.*, 41:2195–2212, 2001.

[20] L. Piegl and W. Tiller. *The NURBS book*. Springer monographs in visual communication, 1997.

[21] E. J. A. Armarego and R. C. Withfield. Computer based modelling of popular machining operations for force and power predictions. *CIRP Annals*, 34(1):65–69, 1985.

[22] T. Insperger, B.P. Mann, G. Stepan, and P.V. Bayly. Stability of up-milling and down-milling, part 1: Alternative analytical methods. *Int. J. Mach. Tools Manuf.*, 43:25–34, 2003.